

**Atomistic Modeling Project**

**Molecular dynamics simulations of  
dislocation motion**

**Bin Wen**

## 1. Project Background

In material science, a dislocation is a crystallographic defect or irregularity within a crystal structure. It defines a great number of properties of crystalline materials, such as yield and flow stress, creep and fatigue, ductility and brittleness, indentation hardness and friction, etc. To study the mechanical behavior of crystalline materials, it is important to understand the mechanism and evolution of dislocations.

Molecular Dynamics (MD), a method directly simulates the “true” dynamics of atoms, can provide unique insights into the mechanistic and quantitative aspects of dislocation mobility. A series of atomistic model are built in this project providing investigations on dislocation evolution and corresponding physical properties. We first introduce a dislocation loop into a perfect FCC crystal, which forms a classical Frank-Read source. Applying shear stress on the slip plane, the mobile dislocation segments bow out. The dissociation of a perfect dislocation line and stacking faults are observed. Then, a study of edge dislocation motion in a BCC metal, Molybdenum, at finite temperature is conducted. The complete simulation includes a relaxation process to minimize the energy at zero temperature, a NVE simulation to reach the thermal equilibrium at a finite temperature, and a NVT simulation to catch the dislocation motion. The relationship between velocity and applied stress is extracted, providing prediction on the flow resistance in the crystal. Several data of drag coefficient are also collected at different temperatures. Finally, an example concerning screw dislocation dipole in Mo is demonstrated. The Peierls stress in relation with geographic factors is analyzed.

## 2. Fundamental dislocation concepts and theories

Before the simulation, a few fundamental concepts need to be explained to show a general picture of dislocation. Some of these items will be defined in the input file of MD model and some of them will be observed during simulation.

### 2.1 Burgers vector, line sense and dislocation types

Dislocations are local discontinuities in the crystal lattice and usually can be thought of as extra lattice planes inserted in the crystal that do not extend through all of the crystal, but end in the dislocation line (Fig.1 (a)). Two important properties of dislocation are (1) line sense (or line direction)  $\xi$ , a direction running along the bottom of the extra half plane, and (2) the Burgers vector  $\mathbf{b}$ , which describes the magnitude and direction of distortion to the lattice (Fig.1 (a)). Based on the relationship between Burgers vector and line sense, two primary dislocation types are determined. An edge dislocation is a defect where an extra half-plane of atoms is introduced mid way through the crystal, distorting nearby planes of atoms as shown in Fig.1 (a). The Burgers vector is perpendicular to the line sense. The second type is screw dislocation, where the Burgers vector is parallel to the line sense. The atoms in this case are arranged in a

spiral around the dislocation line, shown in Fig.1 (b). Combining these two basic types, a dislocation with orientation between screw and edge is called mixed dislocation, shown in Fig.1 (c).

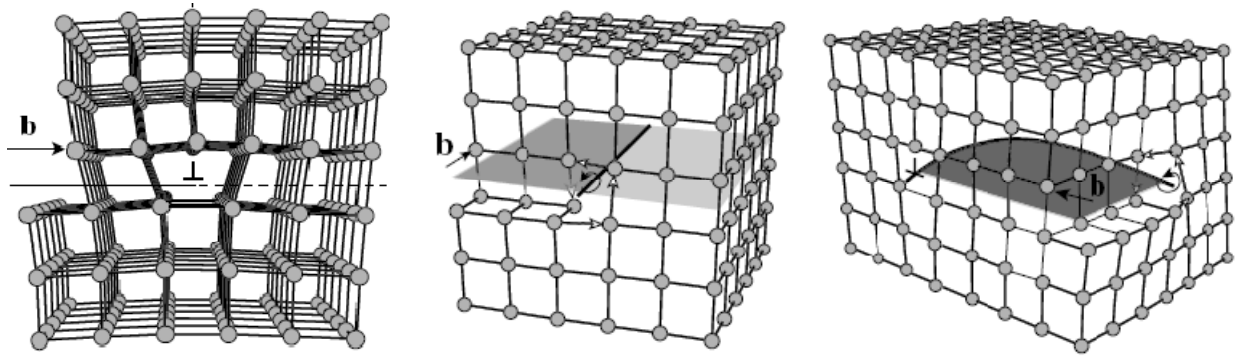


Fig.1 (a) Edge dislocation

(b) screw dislocation

(c) mixed dislocation

## 2.2 Atomistic mechanisms of dislocation motion

In crystal materials, dislocations are able to move under driven force or thermal effects. When the crystal is subjected to an applied stress, dislocation motion provides a mechanism for a crystal to deform plastically, or yield. The intrinsic lattice resistance to dislocation motion is determined by two fundamental parameters: the Peierls barrier, the energy barrier that a dislocation must surmount to move from one preferred position to an adjacent one under zero stress, and the Peierls stress, the ideal critical stress that can make a straight dislocation move at zero temperature. Generally, if the Peierls stress is low (FCC and some BCC metals), dislocations are more likely to move and MD model is well suited to this case.

## 2.3 Frank-Read source

To generate dislocation, a source is needed at the first place. Frank-Read source is such a general multiplication mechanism of dislocation. Consider a dislocation in a crystal slip plane with two ends pinned. If a shear stress is exerted on the slip plane and exceeds the critical value (i.e. Peierls stress), the dislocation segment will become unstable and bow out, leading to the regenerative emission of dislocation loops. The two pinned points generating dislocations are called Frank-Read source. The dislocation bowing and multiplication are schematically illustrated in Fig. 2.

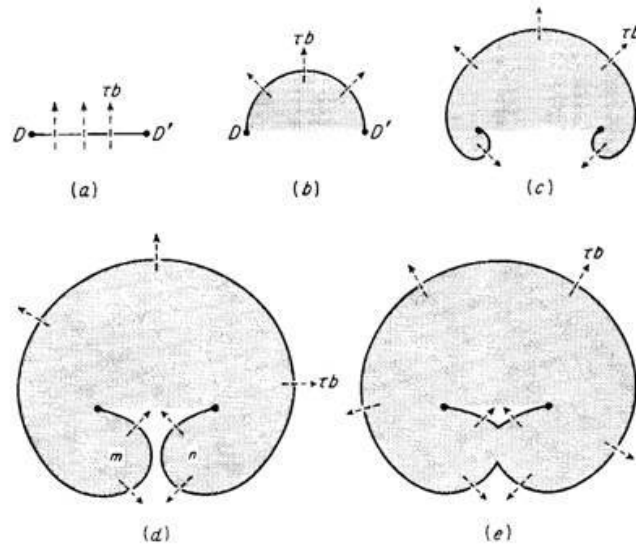


Fig.2 Schematic representation of the operation of a Frank-Read source. A straight dislocation segment is bowed out by the driving shear stress with two pinning points. After a loop forms, a new dislocation segment is born.

### 3. MD simulations

In this section, several MD examples for dislocations are demonstrated. Several methods adopted in the simulation will be explained, while the results are analyzed to give an atomic insight into the dislocation motion. All the simulations in this section are conducted using MD++ code from Wei Cai at Stanford University.

#### 3.1 Frank-Read source, Shockley partials and stacking faults

To be started, we examine a dislocation evolution in aluminum crystal where Frank-Read sources are introduced. The Frank-Read sources, known as a pair of pinning points on slip plane, can be created by removing a rectangular plate of atoms on a  $(-1\ 1\ 0)$  plane. This remove generates a dislocation loop with two segments lying on  $(111)$  planes and two segments on  $(112)$  planes. As we already know that the slip system in FCC crystals are  $\langle 110 \rangle (111)$ , those two segments on the  $(111)$  slip planes are the mobile segments, while the other two perpendicular to the slip plane are immobile which forms two fixed Frank-Read sources. To construct the MD model, first we build a perfect lattice with three orthogonal axes lying in  $[-1\ 1\ 0]$ ,  $[1\ 1\ 1]$  and  $[1\ 1\ -2]$  directions. Then a dislocation loop can be obtained by moving a  $(-1\ 1\ 0)$  plane containing one layer of atoms away from the bulk. Relax the system; a pair of stacking faults bounded by partial dislocations comes into the picture. The dissociate of the burgers vector is presented by

$$\mathbf{b}_1 = \mathbf{b}_2 + \mathbf{b}_3$$

$$\frac{1}{2}[\bar{1}10] = \frac{1}{6}[\bar{2}11] + \frac{1}{6}[\bar{1}2\bar{1}]$$

The reason for this phenomenon is that in the FCC crystal, a pure dislocation state is in a higher energy level than two partial edge dislocations. When the lattice is relaxed, atoms tend to move to positions which render the system total energy minimized. Thus, a pure dislocation will split into two partial dislocations (Shockley partials) in the slip plane. The area between the two partial dislocation lines has a different lattice configuration from the rest parts and is actually a stacking fault area. The schematic illustration of this procedure is shown in Fig.3 and the simulation snapshots are shown in Fig.4. Here we use Conjugate Gradient Relaxation (CGR) algorithm to relax the system. It searches minimum energy in directions conjugate to all previously searched directions. This method works efficient and best in an idealized situation when the potential energy is a quadratic function. But we still keep in mind that it is a method that search for local minimum energy but not global, which can be found with the assistance of simulated annealing.

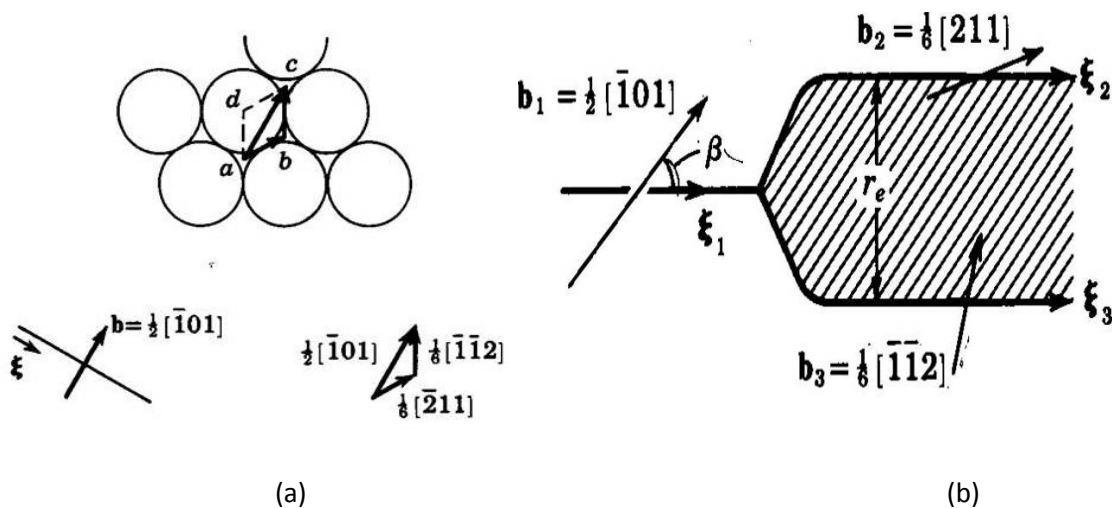


Fig.3(a) Atoms on the bottom side of a (1 1 1) glide plane. A perfect  $\frac{1}{2}[\bar{1}01]$  dislocation splits into two Shockley partial dislocations. (b) Dissociation of a perfect dislocation into Shockley partials. The shade area represents stacking fault.

When the dislocation loop is formed, the Frank-Read source can be activated by exerting shear stress along slip direction  $[-1 1 0]$  on the slip plane (1 1 1). As two dislocation segments lying on (1 1 1) planes are easy to move while the movement of other two segments (lying on (1 1 -2) planes) are difficult. The mobile segments will bow out with two pinning points formed by the immobile segments under applied stress. An area of stacking fault bounded by two partial dislocations can be observed in Fig.4.

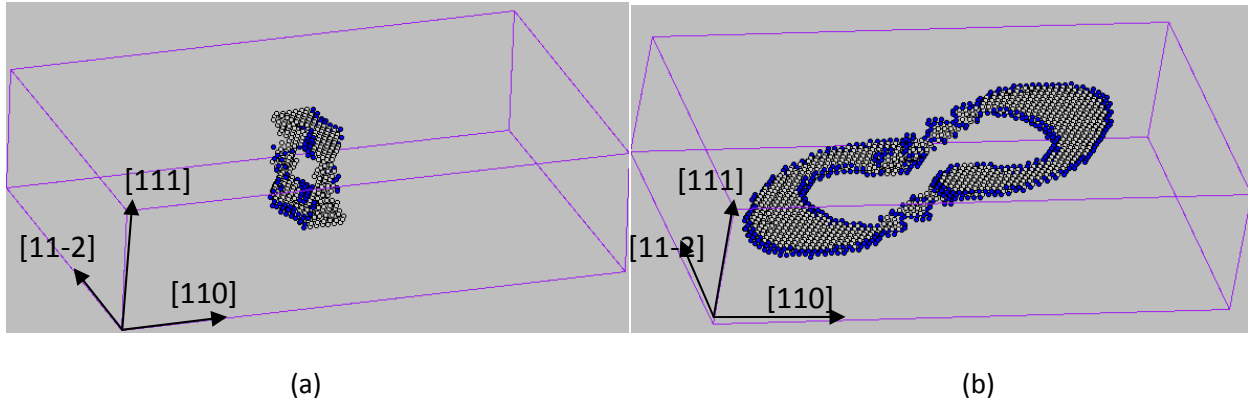


Fig.4 (a) A Dislocation loop created by removing a plate of atoms out of the perfect crystal. Two dislocation segments lie on (1 1 1) planes are movable while the other two segments lie on (1 1 -2) planes are fixed behaving as the Frank-Read sources. (b) Stacking fault bounded by two bowing out partial dislocations. These defects are identified according to the CSD parameter of each atom. The blue atoms are the partial dislocation cores and the gray atoms represent stacking faults.

The above two pictures are plotted with respect to centro-symmetry deviation (CSD) parameters, which quantitatively measures the deviation from the ideal centro-symmetry in a given atom's neighborhood. This method is very effective in a center symmetric crystal where the energy difference between defect cores and perfect crystal are slight.

### 3.2 MD simulation of BCC crystal dislocation motion at finite temperature

In section 3.1, the formation of Frank-Read source and stacking faults in FCC crystal at zero temperature is studied, giving us a general picture of dislocation simulation using MD. To expand our repertoire, a complete edge dislocation motion at finite temperature is simulated in the background of BCC metal. The dependence of dislocation velocity on applied stress and the relationship between drag coefficient  $B$  and temperature will be analyzed.

First, we need to build a simulation cell. Instead of moving a half plane out of a cell, here we construct two separate rectangular slabs of molybdenum atoms and stack one on top of the other. The upper slab has dimensions  $L_x1=30/2[1\ 1\ 1]$ ,  $L_y1=10[-1\ 0\ 1]$ ,  $L_z1=8[1\ -2\ 1]$ . The lower slab with dimensions  $L_x2=29/2[1\ 1\ 1]$ ,  $L_y2=10[-1\ 0\ 1]$ ,  $L_z2=8[1\ -2\ 1]$  is one layer thinner than the upper. Both of them has lattice constant  $a=3.1472$  Angstroms. Join two crystals along their  $x$ - $z$  faces and make both of them have the same length,  $L_x=29.5[1\ 1\ 1]/2$ , in  $x$  direction. A bi-crystal with a misfit interface on the horizontal mid-plane is obtained and shown in Fig.5 (a). Periodic boundary conditions are applied along the line direction ( $z$  axis) and the direction of dislocation motion ( $x$  axis). The boundary of the direction perpendicular to the slip plane ( $y$  axis) is fixed. Then relax the atoms so that they can adjust their position to reach the minimum energy state at zero temperature.

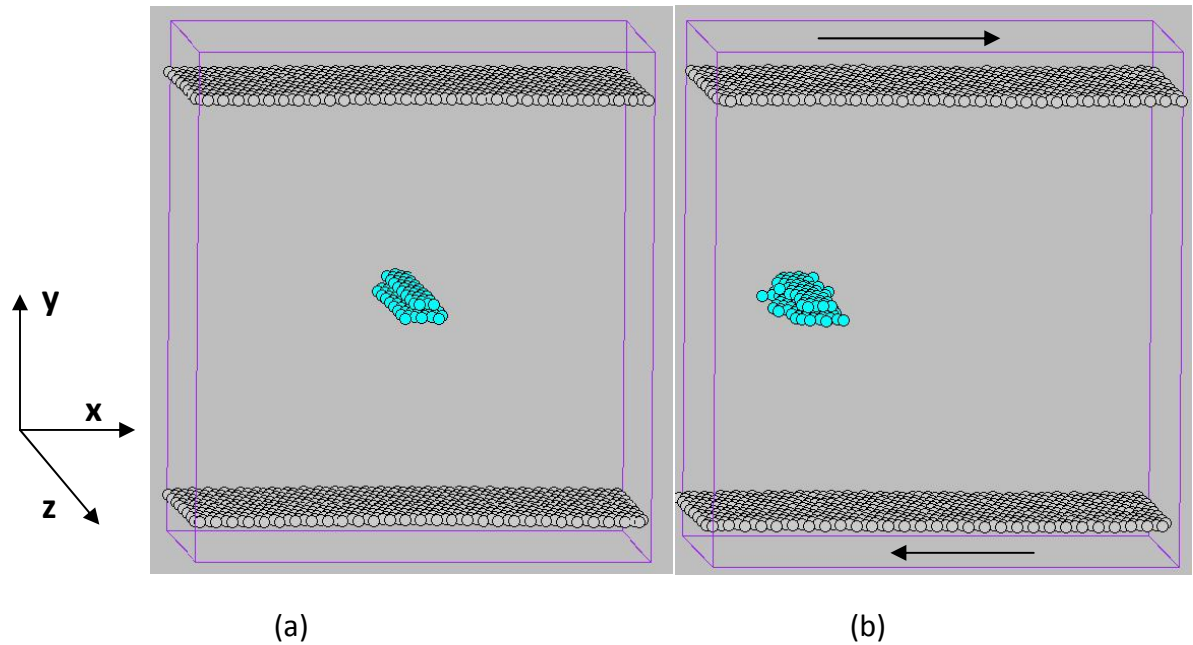
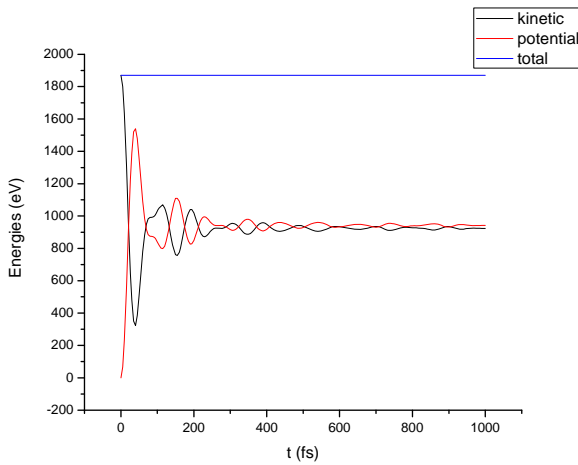
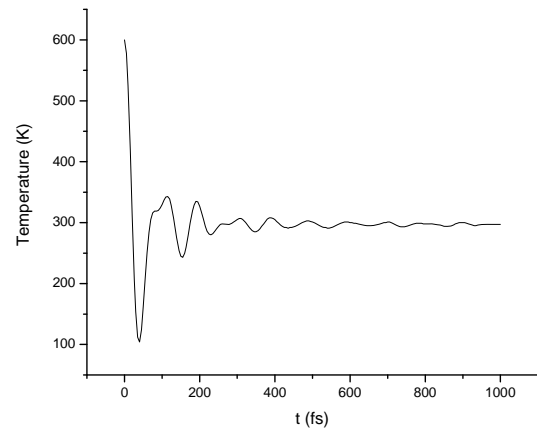


Fig. 5 (a) The simulation cell with an edge dislocation on the interface of bi-crystal. (b) A snapshot of dislocation motion. The velocity of dislocation is to the right. This picture shows the dislocation went out of the cell on the right side and then reentered from the left side. Only the atoms with CSD parameter larger than  $1.5\text{\AA}^2$  are plotted. The cyan balls indicate dislocation core; the gray balls are the boundaries outside which no atom exist.

To prepare this atomistic configuration for subsequent dislocation motion simulation, we would like to bring the system to a state of thermal equilibrium at a finite temperature. Taking 300K as an example, first we initialize each atom with a random velocity making sure that the total kinetic energy renders a temperature around 600K. Then, we let the atoms move following Newton's law and interact with each other. After some period of time, the MD simulation can bring the system to a state of thermal equilibrium where the distribution of velocity obeys Boltzmann's distribution and the temperature should fluctuate around the target temperature 300K with mild amplitude. In this process, total energy, the number of atoms and the cell volume are preserved (NVE). The system is in a microstate corresponding to a micro-canonical ensemble. In this example, Finnis-Sinclair potential function, a type of EAM potential, is used here and approximated by a harmonic function provided that the atomic positions are not too far away from the local minimum. The energies and temperature with respect to time during equilibrium run are plotted in Fig. 6.



(a)



(b)

Fig.6 (a) Kinetic energy (black), potential energy (red) and total energy (blue), as a function of time (in femtoseconds). The reference potential energy is set to be -162851.82 eV. (b) The instantaneous temperature as a function of time gradually settles to 300K.

Fig.6 (a) reveals a vigorous exchange between the kinetic and the potential energies over the first 400 fs corresponding to large fluctuation of the instantaneous temperature shown in Fig.6 (b). Since the temperature is initialized at 600K (double of the target temperature), the kinetic energy is at its maximum value at the beginning, while the potential energy is 0. When the temperature fluctuates to 300K, the kinetic energy decreases with fluctuation and the potential energy increases keeping the total energy conserved.

The total Hamiltonian is

$$H(\{\mathbf{r}_i, \mathbf{p}_i\}) = \sum_{i=1}^N \frac{|\mathbf{p}_i|^2}{2m} + V(\{\mathbf{r}_i\}).$$

After about  $t=600$  fs, the amplitude of fluctuations decreases gradually. The system approaches thermal equilibrium where the average potential energy is equal to average kinetic energy. This is a direct result of the harmonic system, where the potential  $V(\{\mathbf{r}_i\})$  is a quadratic function of the atomic positions. Both the average kinetic energy and potential energy is  $U=3/2Nk_B T$ .

Having obtained atomistic equilibrated configuration at 300K, we are ready to apply shear stresses on the simulation cell, which produce the driven force on dislocation. Here we applied stress  $\sigma_{xy}$  with magnitude 300Mpa on both surfaces. The total force is 9.287 eV/Å. Recall that the upper box has one more layer of atoms than the lower box. The top surface contains more atoms than the bottom surface (720 versus 696). Therefore, the force per atom  $f_x$  is difference

on the two boundaries: on the top surface  $f_x=0.01290$  eV/A; on the bottom surface,  $f_x=-0.01334$  eV/A. In the simulation of dislocation motion, we need the temperature stays close to 300K. However the work done by external forces will be dissipated as heat which will inevitably raise the temperature obtained in the equilibrium run unless some mechanism to remove heat is adopted. An obvious way to maintain a constant temperature is to rescale the atomic velocities at periodic intervals during the simulation. The method we used in this project is Nose-Hoover thermostat, which mimics heat exchange between a simulation volume and its surroundings. As temperature maintains a constant temperature, a canonical or NVT ensemble is resulted. Fig.5 (b) demonstrates a location of moved dislocation at certain time step. Given periodic boundary condition in x direction, the dislocation will come into the simulation cell from the left side when it goes out of the box from the right side.

In order to analyze the dependence of dislocation velocity on applied stress, the primary task is to extract instantaneous dislocation position at each time step. The CSD parameter offers us an effective way to do that. Here we define the dislocation core the atoms whose CSD falls in the range between  $1.5 \text{ \AA}^2$  and  $10 \text{ \AA}^2$ , leaving non-core atoms as those possessing CSD less than  $1.5 \text{ \AA}^2$ . Thus the position of dislocation can be determined by finding the mean location of core atoms at specific time. The dislocation position corresponding to time is depicted in Fig. 7 (a). We can see that the dislocation moves linearly with time increment after a short period. Linear fit the data when the dislocation motion is steady and find the slope of the straight fitting line. It is convenient to get a constant velocity under specific stress. For the case at temperature 300K and shear stress 300 Mpa, the velocity is approximately 1176 m/s.

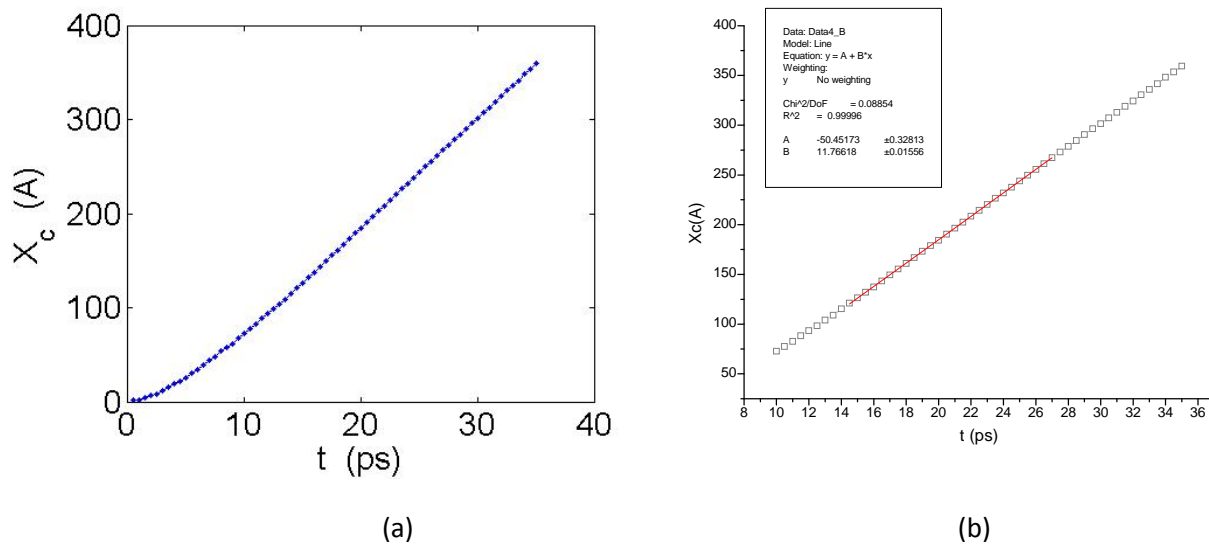


Fig.7 (a) Dislocation position as a function of time at temperature equal to 300K and shear stress equal to 300Mpa. (b) A linear fit of dislocation positions when  $t>10$ ps. The slope indicates a constant velocity, 1176 m/s, of dislocation motion.

Varying applied shear stress, a series of MD simulations are conducted in the spirit of finding the dependence of dislocation velocity on stress. The same procedure of extracting velocity is adopted as before. The dislocation velocity as a function of time is depicted in Fig.8 (a) within the stress range from 50 Mpa to 300 Mpa. A linear dependence of dislocation velocity is shown, providing a measure of viscous drag coefficient  $B = \sigma b / v$ . At different temperature,  $B$  changes correspondingly (Fig. 8 (b)), indicating the velocity dependence on applied stress varies. This information about drag coefficient can be used to construct mobility functions for dislocation dynamics which deals with a large amount of dislocations interacting with each other. It leads to a hierarchical multiscale modeling methodology bridging the nanoscale and microscale.

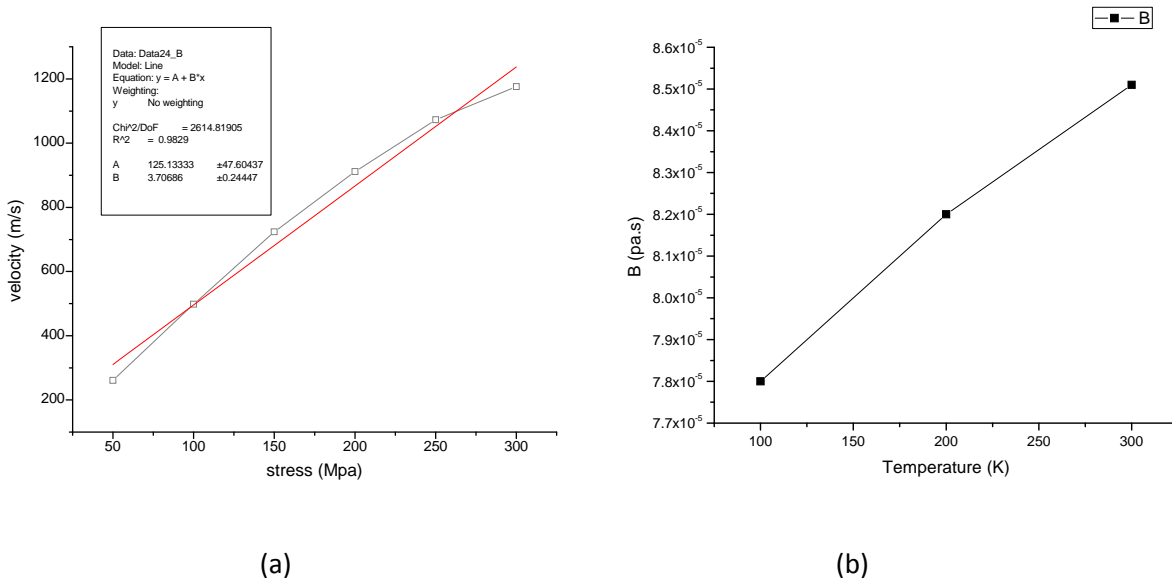


Fig.8 (a) Stress dependence of edge dislocation velocity in Mo. The gray points are MD estimated data and the red line is a linear fit of the data. (b) Temperature dependence of drag coefficient for edge dislocation in Mo.

From the Fig.8 (a), we find that the dislocation velocity increases when the applied stress becomes larger. The picture shows a diminishing trend of this increase, but still, this relationship can be approximately represented by a linear law (within the range from 50Mpa to 300Mpa). Collecting velocity-stress relationship at different temperatures, drag coefficient can be estimated using  $B = \sigma b / v$ . Because each computation of  $B$  needs a bunch of calculations of  $v$ - $s$  curve, the consumption is very expansive. Here we only calculate 3 points for  $B$  at the temperature of 100K, 200K and 300K. Fig.8 (b) can give us a conceptual idea of the dependence of  $B$  on temperature:  $B$  increases along with temperature.

### 3.3 Screw dislocation dipole in BCC metal

In this section, we study a screw dislocation example and calculate its Peierls stress ( $\tau_p$ ), the stress necessary to move a dislocation at zero temperature. A perfect BCC (Ta) lattice with three orthogonal dimensions  $\mathbf{c1}=8[1\ 1\ -2]$ ,  $\mathbf{c2}=19[1\ -1\ 0]$  and  $\mathbf{c3}=5/2[1\ 1\ 1]$  is constructed first. Periodic boundary conditions are applied in all the three directions. As a fully periodic simulation cell can accommodate only dislocation arrangements whose net Burgers vector is zero, the minimal number of dislocations need to be introduced in the simulation cell is two. Here we introduce a dislocation dipole into the perfect BCC crystal structure by displacing the atoms immediately on top of cut plane **A** by a Burgers vector (**b**) with respect to the atoms below the cut. The dipole is positioned perpendicular to the glide plane (1 -1 0), as shown in Fig.9 (a), to avoid the recombination of dislocations. The simulation cell needs to adjust its shape in order to compensate for the internal stress produced by dislocations. Then relax the atoms using CGR to minimize the energy.

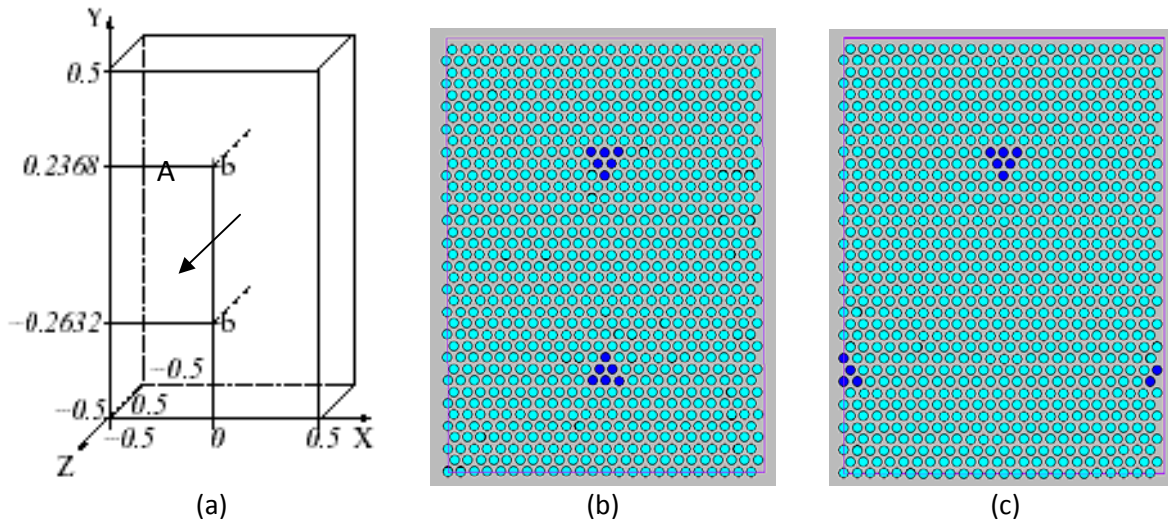


Fig.9 (a) Schematic representation of simulation cell with a dislocation dipole inside it. (b) MD model with the distance between to dislocations along motion direction is 0. (c) MD model with the distance between to dislocations along motion direction is  $c1/2$ .

After the preparation work is done, we apply a constant stress  $\sigma_{yz}$  into the structure. This stress exerts equal but opposite forces on the two dislocations in the  $\mathbf{y}$  and  $-\mathbf{y}$  directions, respectively. The magnitude of this stress is gradually increased until a critical stress ( $\tau_c$ ), at which dislocations begin to move, is achieved. This critical stress can be treated as the Peierls stress somehow. However, it does not necessarily equal the Peierls stress because of possible effects of the boundary image forces. It is proved [1] that if the distance ( $\mathbf{d}$ ) between the two dislocations along their motion direction  $\mathbf{x}$  ( $1\ 1\ -2$ ) is zero (Fig.9 (b)),  $\tau_c$  overestimates  $\tau_p$ ; in contrast, when  $\mathbf{d}=\mathbf{c1}/2$  (Fig.9 (c)),  $\tau_c$  underestimates  $\tau_p$ . Thus, we can estimate the Peierls stress by averaging the  $\tau_c$  calculated in the two situations to cancel out the errors. Varying the ratio of  $\mathbf{c2}/\mathbf{c1}$ ,  $\tau_c$  in both cases converges to a specific value, 2.10 Gpa for Ta, as  $\mathbf{c2}$  increases keeping  $\mathbf{c1}$  constant. This value is a little different from the date given in reference [1], maybe because  $\mathbf{c1}=5[1\ 1\ -1]$  in their example.

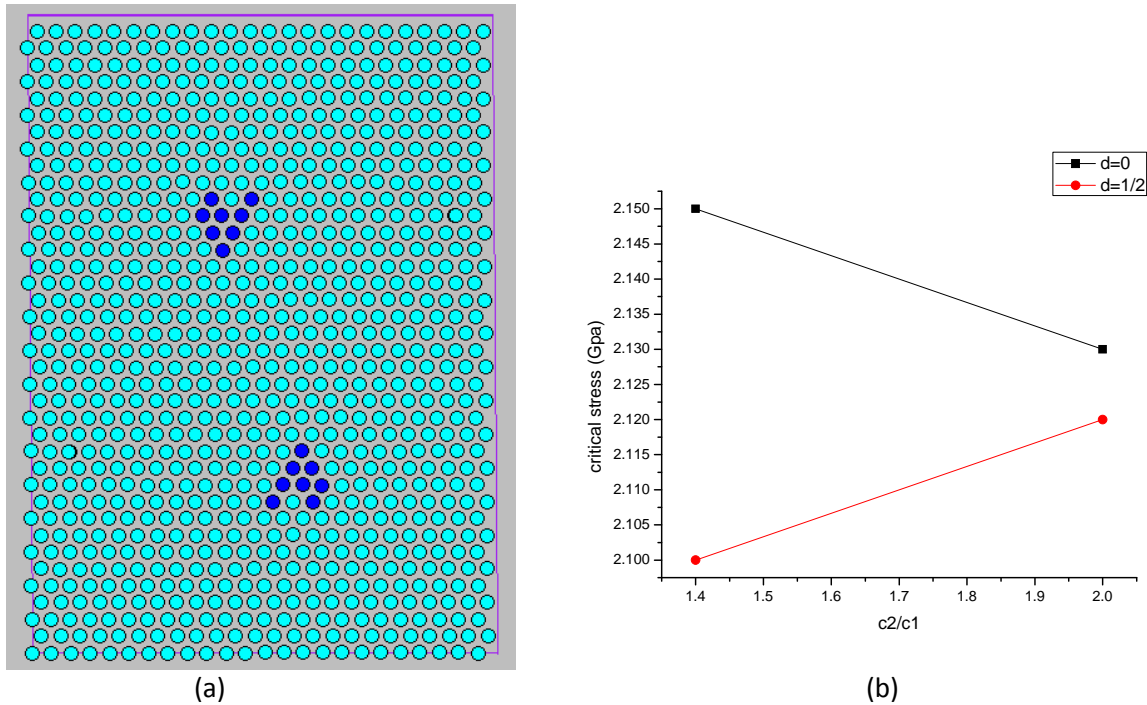


Fig. 10 (a) MD model when the dislocations of a dipole moves, indicating the exerting stress overwhelms the critical stress. (b) Critical stress computed in simulation cell with different ratios of  $c2/c1$  at fixed  $c1$ . (Only two set of data are collected due to the limit capability of the code. When the cell becomes big, the MD cannot handle it. )

#### 4. Summary

A series of dislocation studies are carried out using molecular dynamics simulation. From the first example, we successfully observed dislocation bowing out with two pinning Frank-Read sources and the stacking faults bounded by two dissociated partial dislocations. In the second example, a complete case of dislocation motion under driving forces at a finite temperature is studied. The motion of dislocation is observed and the dependence of velocity on applied stress is extracted. The results show that in BCC Mo, the dislocation velocity increases with increasing shear stress within the range of [50Mpa, 300Mpa]. Although the increasing rate of the velocity becomes slower as stress rises, we can still obtain a nearly linear relationship between them. Some data about drag coefficient are also collected. Because of the heavy cost of running an example, the data is very limit, giving only a general idea that drag coefficient goes up with increasing temperature in Mo. In the last example, screw dislocations dipole is built in a BCC crystal Ta. Periodic boundary conditions are assigned in all the three dimensions. The Peierls stress is analyzed by observing the movement of the dislocation.

## Reference

- [1] Vasily V. Bulatov and Wei Cai, *Computer Simulations of Dislocations*, Oxford University Press, Oct 2006.
- [2] J. Chang, Wei Cai, V. V. Bulatov and S. Yip, "[Dislocation Motion in BCC Metals by Molecular Dynamics](#)", *Materials Science and Engineering A*, 309-310, 160 (2001).
- [3] J. Chang, Wei Cai, V. V. Bulatov, and S. Yip, "[Molecular Dynamics Simulations of Motion of Edge and Screw Dislocations in a Metal](#)", *Computational Materials Science*, 23, 111, (2002).
- [4] H.P. Hirth and J Lothe, "Theory of Dislocations", A Wiley-Interscience publication, 1982